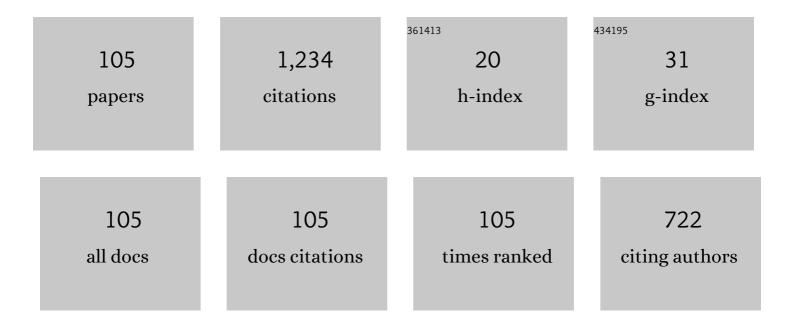
Nektarios Kalyvas

List of Publications by Year in descending order

Source: https://exaly.com/author-pdf/6822548/publications.pdf Version: 2024-02-01



#	Article	IF	CITATIONS
1	Cerium Bromide Single-Crystal X-Ray Detection and Spectral Compatibility Assessment with Various Optical Sensors. Material Design and Processing Communications, 2022, 2022, 1-7.	0.9	2
2	Efficiency Properties of Cerium-Doped Lanthanum Chloride (LaCl3:Ce) Single Crystal Scintillator under Radiographic X-ray Excitation. Crystals, 2022, 12, 655.	2.2	6
3	Study of UV interactions on PMMA based ZnCuInS/ZnS quantum dot films. Optical Materials, 2022, 129, 112493.	3.6	1
4	Temperature dependence of ZnSe:Te scintillator. Procedia Structural Integrity, 2022, 41, 82-86.	0.8	1
5	Luminescence Efficiency of Cerium Bromide Single Crystal under X-ray Radiation. Crystals, 2022, 12, 909.	2.2	4
6	RAD_IQ: A free software for characterization of digital X-ray imaging devices based on the novel IEC 62220-1-1:2015 International Standard. Journal of Physics: Conference Series, 2021, 2090, 012107.	0.4	1
7	On the thermal response of LuAG:Ce single crystals. Procedia Structural Integrity, 2021, 33, 287-294.	0.8	3
8	Spatial frequency domain analysis of a commercially available digital dental detector. Measurement: Journal of the International Measurement Confederation, 2020, 151, 107171.	5.0	3
9	MTF of columnar phosphors with a homogenous part: an analytical approach. Medical and Biological Engineering and Computing, 2020, 58, 2551-2565.	2.8	0
10	On the Optical Response of Tellurium Activated Zinc Selenide ZnSe:Te Single Crystal. Crystals, 2020, 10, 961.	2.2	14
11	Poly(Methyl Methacrylate) Structure Modification through Zn-Cu-In-S / ZnS Quantum Dot Nanocrystals Dispersion. Procedia Structural Integrity, 2020, 25, 47-54.	0.8	1
12	Luminescence efficiency of CaF2:Eu single crystals: Temperature dependence. Procedia Structural Integrity, 2020, 26, 3-10.	0.8	9
13	Spectral efficiency of lutetium aluminum garnet (Lu3Al5O12:Ce) with microelectronic optical sensors. Microelectronics Reliability, 2020, 109, 113658.	1.7	5
14	Luminescence Efficiency of Cadmium Tungstate (CdWO4) Single Crystal for Medical Imaging Applications. Crystals, 2020, 10, 429.	2.2	26
15	Temperature Dependence of the Luminescence output of CdWO4 Crystal. Comparison with CaF2:Eu. Procedia Structural Integrity, 2020, 28, 971-977.	0.8	5
16	Optical Characteristics of ZnCuInS/ZnS (Core/Shell) Nanocrystal Flexible Films Under X-Ray Excitation. Crystals, 2019, 9, 343.	2.2	18
17	Luminescence Efficiency of Zn-Cu-In-S / ZnS Quantum Dot films. , 2019, , .		3
18	Information Content in Nuclear Medicine Imaging. Energy Procedia, 2019, 157, 1517-1524.	1.8	2

#	Article	IF	CITATIONS
19	Analytical and Monte Carlo comparisons on the optical transport mechanisms of powder phosphors. Optical Materials, 2019, 88, 396-405.	3.6	2
20	Fabrication and Luminescent Properties of Zn–Cu–In–S/ZnS Quantum Dot Films under UV Excitation. Applied Sciences (Switzerland), 2019, 9, 2367.	2.5	8
21	Absolute Luminescence Efficiency of Europium-Doped Calcium Fluoride (CaF2:Eu) Single Crystals under X-ray Excitation. Crystals, 2019, 9, 234.	2.2	25
22	Luminescence efficiency of calcium tungstate (CaWO4) under X-ray radiation: Comparison with Gd2O2S:Tb. Measurement: Journal of the International Measurement Confederation, 2018, 120, 213-220.	5.0	36
23	Information Capacity of Positron Emission Tomography Scanners. Crystals, 2018, 8, 459.	2.2	12
24	Detective quantum efficiency (DQE) of high X-ray absorption Lu2O3:Eu thin screens: the role of shape and size of nano- and micro-grains. Applied Physics A: Materials Science and Processing, 2018, 124, 1.	2.3	5
25	Grains size and shape dependence of luminescence efficiency of Lu2O3:Eu thin screens. Results in Physics, 2017, 7, 980-981.	4.1	8
26	Detective quantum efficiency (DQE) in PET scanners: A simulation study. Applied Radiation and Isotopes, 2017, 125, 154-162.	1.5	15
27	An analytical approach to the light transport in columnar phosphors. Detector Optical Gain, angular distribution and the CsI:Tl paradigm. Physica Medica, 2017, 35, 39-49.	0.7	3
28	Dual energy subtraction method for breast calcification imaging. Nuclear Instruments and Methods in Physics Research, Section A: Accelerators, Spectrometers, Detectors and Associated Equipment, 2017, 848, 31-38.	1.6	17
29	Preliminary Study of ZnS:Mn ²⁺ Quantum Dots Response Under UV and X-Ray Irradiation. Journal of Physics: Conference Series, 2017, 931, 012030.	0.4	4
30	X-ray imaging resolution of phosphor screens prepared with different grains size and shape of granular Lu ₂ O ₃ :Eu. Journal of Physics: Conference Series, 2017, 931, 012032.	0.4	1
31	Infrared thermography quantitative image processing. Journal of Physics: Conference Series, 2017, 931, 012033.	0.4	2
32	Examining the Spatial Frequency Components of a Digital Dental Detector. Journal of Physics: Conference Series, 2017, 931, 012005.	0.4	0
33	3D printing X-Ray Quality Control Phantoms. A Low Contrast Paradigm. Journal of Physics: Conference Series, 2017, 931, 012026.	0.4	3
34	Resolution Properties of a Calcium Tungstate (CaWO ₄) Screen Coupled to a CMOS Imaging Detector. Journal of Physics: Conference Series, 2017, 931, 012027.	0.4	3
35	X-ray response of a digital detector for dental radiographs. Physica Medica, 2016, 32, 286-287.	0.7	1
36	Detective quantum efficiency (DQE) of the Dexela 2923MAM detector according to IEC 62220-1-1:2015. Physica Medica, 2016, 32, 291-292.	0.7	2

#	Article	IF	CITATIONS
37	Determination of the detective quantum efficiency (DQE) of CMOS/CsI imaging detectors following the novel IEC 62220-1-1:2015 International Standard. Radiation Measurements, 2016, 94, 8-17.	1.4	44
38	Investigating the particle packing of powder phosphors for imaging instrumentation technology: an examination of Gd ₂ O ₂ S:Tb phosphor. Journal of Instrumentation, 2016, 11, P10001-P10001.	1.2	8
39	On the response of semitransparent nanoparticulated films of LuPO4:Eu in poly-energetic X-ray imaging applications. Applied Physics A: Materials Science and Processing, 2016, 122, 1.	2.3	15
40	Evaluation of Gd2O2S:Pr granular phosphor properties for X-ray mammography imaging. Journal of Luminescence, 2016, 169, 706-710.	3.1	19
41	A novel method for the optimization of positron emission tomography scanners imaging performance. Hellenic Journal of Nuclear Medicine, 2016, 19, 231-240.	0.3	11
42	A theoretical investigation of spectra utilization for a CMOS based indirect detector for dual energy applications. Journal of Physics: Conference Series, 2015, 633, 012095.	0.4	0
43	Optimum filter selection for Dual Energy X-ray Applications through Analytical Modeling. Journal of Physics: Conference Series, 2015, 633, 012093.	0.4	Ο
44	Modeling indirect detectors for performance optimization of a digital mammographic detector for dual energy applications. Journal of Physics: Conference Series, 2015, 574, 012075.	0.4	2
45	Modeling of the Calcium/Phosphorus Mass ratio for Breast Imaging. Journal of Physics: Conference Series, 2015, 633, 012094.	0.4	4
46	Medical Imaging Image Quality Assessment with Monte Carlo Methods. Journal of Physics: Conference Series, 2015, 633, 012096.	0.4	1
47	Pencil Beam Spectral Measurements of Ce, Ho, Yb, and Ba Powders for Potential Use in Medical Applications. Journal of Spectroscopy, 2015, 2015, 1-8.	1.3	9
48	Dual Energy Method for Breast Imaging: A Simulation Study. Computational and Mathematical Methods in Medicine, 2015, 2015, 1-8.	1.3	19
49	Preparation and imaging performance of nanoparticulated LuPO4:Eu semitransparent films under x-ray radiation. , 2015, , .		Ο
50	A theoretical study of CsI:Tl columnar scintillator image quality parameters by analytical modeling. Nuclear Instruments and Methods in Physics Research, Section A: Accelerators, Spectrometers, Detectors and Associated Equipment, 2015, 779, 18-24.	1.6	13
51	Experimental measurement of a high resolution CMOS detector coupled to CsI scintillators under X-ray radiation. Radiation Measurements, 2015, 74, 39-46.	1.4	36
52	Luminescence efficiency of (Lu,Gd)2SiO5:Ce (LGSO:Ce) crystals under X-ray radiation. Radiation Measurements, 2015, 80, 1-9.	1.4	8
53	Optimization of breast cancer detection in Dual Energy X-ray Mammography using a CMOS imaging detector. Journal of Physics: Conference Series, 2015, 574, 012076.	0.4	1
54	Measuring scatter radiation in diagnostic X rays for radiation protection purposes. Radiation Protection Dosimetry, 2015, 165, 382-385.	0.8	15

#	Article	IF	CITATIONS
55	A Novel Method for the Image Quality assessment of PET Scanners by Monte Carlo simulations: Effect of the scintillator. Journal of Physics: Conference Series, 2014, 490, 012139.	0.4	4
56	Figure of Image Quality and Information Capacity in Digital Mammography. BioMed Research International, 2014, 2014, 1-11.	1.9	14
57	Comparing analytical and Monte Carlo optical diffusion models in phosphor-based X-ray detectors. Proceedings of SPIE, 2014, , .	0.8	1
58	Imaging performance of a thin Lu2O3:Eu nanophosphor scintillating screen coupled to a high resolution CMOS sensor under X-ray radiographic conditions: comparison with Gd2O2S:Eu conventional phosphor screen. , 2014, , .		1
59	Measurement of the luminescence properties of Gd2O2S:Pr,Ce,F powder scintillators under X-ray radiation. Radiation Measurements, 2014, 70, 59-64.	1.4	38
60	Light emission efficiency and imaging performance of Lu2O3:Eu nanophosphor under X-ray radiography conditions: Comparison with Gd2O2S:Eu. Journal of Luminescence, 2014, 151, 229-234.	3.1	41
61	Studying the energy dependence of intrinsic conversion efficiency of single crystal scintillators under X-ray excitation. Optics and Spectroscopy (English Translation of Optika I Spektroskopiya), 2014, 116, 743-747.	0.6	5
62	Light Emission Efficiency of Gd3Al2Ga3O12:Ce (GAGG:Ce) Single Crystal Under X-ray Radiographic Conditions. IFMBE Proceedings, 2014, , 455-458.	0.3	2
63	On the response of a europium doped phosphor-coated CMOS digital imaging detector. Nuclear Instruments and Methods in Physics Research, Section A: Accelerators, Spectrometers, Detectors and Associated Equipment, 2013, 729, 307-315.	1.6	34
64	Light emission efficiency of Lu ₂ O ₃ :Eu nanophosphor scintillating screen under x-ray radiographic conditions. Proceedings of SPIE, 2013, , .	0.8	1
65	On the response of GdAlO3:Ce powder scintillators. Journal of Luminescence, 2013, 144, 45-52.	3.1	40
66	Analysis of the imaging performance in indirect digital mammography detectors by linear systems and signal detection models. Nuclear Instruments and Methods in Physics Research, Section A: Accelerators, Spectrometers, Detectors and Associated Equipment, 2013, 697, 87-98.	1.6	8
67	A semi-empirical Monte Carlo based model of the Detector Optical Gain of Nuclear Imaging scintillators. Journal of Instrumentation, 2012, 7, P11021-P11021.	1.2	9
68	Studying the luminescence efficiency of Lu2O3:Eu nanophosphor material for digital X-ray imaging applications. Applied Physics A: Materials Science and Processing, 2012, 106, 131-136.	2.3	27
69	Thin substrate powder scintillator screens for use in digital X-ray medical imaging applications. , 2011, , , .		0
70	Evaluation of the Red Emitting \${m Gd}_{2}{m O}_{2}{m S}!!:!!{m Eu}\$ Powder Scintillator for Use in Indirect X-Ray Digital Mammography Detectors. IEEE Transactions on Nuclear Science, 2011, 58, 2503-2511.	2.0	24
71	Modeling noise properties of a high resolution CMOS detector for X-ray digital mammography. , 2011, , \cdot		0
72	Experimental and Theoretical Evaluation of a High Resolution CMOS Based Detector Under X-Ray Imaging Conditions. IEEE Transactions on Nuclear Science, 2011, 58, 314-322.	2.0	58

#	Article	IF	CITATIONS
73	Comparison of full field digital (FFD) and computed radiography (CR) mammography systems in Greece. Radiation Protection Dosimetry, 2011, 147, 202-205.	0.8	2
74	Light emission efficiency and imaging performance of powder scintillator under xâ€ray radiography conditions. Medical Physics, 2010, 37, 3694-3703.	3.0	52
75	Imaging performance of a high resolution CMOS sensor under Mammographic and Radiographic conditions. , 2010, , .		0
76	A theoretical model describing the light emission efficiency of single-crystal scintillators in the diagnostic energy range. Journal of Instrumentation, 2009, 4, P06016-P06016.	1.2	3
77	The influence of software filtering in digital mammography image quality. Journal of Instrumentation, 2009, 4, P05018-P05018.	1.2	3
78	Modelling the imaging performance and low contrast detectability in digital mammography. Journal of Instrumentation, 2009, 4, P06004-P06004.	1.2	2
79	Imaging performance and light emission efficiency of Lu2 SiO5:Ce (LSO:Ce) powder scintillator under X-ray mammographic conditions. Applied Physics B: Lasers and Optics, 2009, 95, 131-139.	2.2	18
80	Investigation of two heavy element scintillators by Monte-Carlo methods. Journal of Instrumentation, 2009, 4, P05019-P05019.	1.2	1
81	Evaluating optical spectral matching of phosphor-photodetector combinations. Journal of Instrumentation, 2009, 4, P07003-P07003.	1.2	1
82	A comparative investigation of Lu ₂ SiO ₅ :Ce and Gd ₂ O ₂ S:Eu powder scintillators for use in x-ray mammography detectors. Measurement Science and Technology, 2009, 20, 104008.	2.6	25
83	A comparative investigation of Lu <inf>2</inf> SiO <inf>5</inf> :Ce and Gd <inf>2</inf> O <inf>2</inf> S:Eu phosphor scintillators for use in a medical imaging detectors. , 2008, , .		1
84	Light Emission Efficiency of \${m Gd}_{2} {m O} _{2} {m S}!!!:!!!{m Eu}\$ (GOS:Eu) Powder Screens Under X-Ray Mammography Conditions. IEEE Transactions on Nuclear Science, 2008, 55, 3703-3709.	2.0	18
85	Image quality evaluation and patient dose assessment of medical fluoroscopic X-ray systems: a national study. Radiation Protection Dosimetry, 2007, 129, 419-425.	0.8	3
86	Performance of medical radiographic X-ray systems in Greece for the time period 1998–2004. Physica Medica, 2007, 23, 107-114.	0.7	10
87	A systematic study of the performance of the CsI:Tl single-crystal scintillator under X-ray excitation. Nuclear Instruments and Methods in Physics Research, Section A: Accelerators, Spectrometers, Detectors and Associated Equipment, 2007, 571, 343-345.	1.6	19
88	Efficiency of Lu2SiO5:Ce (LSO) powder phosphor as X-ray to light converter under mammographic imaging conditions. Nuclear Instruments and Methods in Physics Research, Section A: Accelerators, Spectrometers, Detectors and Associated Equipment, 2007, 571, 346-349.	1.6	12
89	Evaluation of high packing density powder X-ray screens by Monte Carlo methods. Nuclear Instruments and Methods in Physics Research, Section A: Accelerators, Spectrometers, Detectors and Associated Equipment, 2007, 580, 427-429.	1.6	1
90	Investigation of the effect of the scintillator material on the overall X-ray detection system performance by application of analytical models. Nuclear Instruments and Methods in Physics Research, Section A: Accelerators, Spectrometers, Detectors and Associated Equipment, 2007, 571, 270-273.	1.6	3

#	Article	IF	CITATIONS
91	Light emission efficiency and imaging properties of YAP:Ce granular phosphor screens. Applied Physics A: Materials Science and Processing, 2007, 89, 443-449.	2.3	20
92	Evaluation of the imaging performance of LSO powder scintillator for use in X-ray mammography. Nuclear Instruments and Methods in Physics Research, Section A: Accelerators, Spectrometers, Detectors and Associated Equipment, 2007, 580, 558-561.	1.6	22
93	Luminescence efficiency of Lu2SiO5:Ce (LSO) powder scintillator for X-ray medical radiography applications. , 2006, , .		1
94	A theoretical model evaluating the angular distribution of luminescence emission in X-ray scintillating screens. Applied Radiation and Isotopes, 2006, 64, 508-519.	1.5	13
95	The effect of energy weighting on the SNR under the influence of non-ideal detectors in mammographic applications. Nuclear Instruments and Methods in Physics Research, Section A: Accelerators, Spectrometers, Detectors and Associated Equipment, 2006, 569, 260-263.	1.6	10
96	Imaging properties of cerium doped Yttrium Aluminum Oxide (YAP:Ce) powder scintillating screens under X-ray excitation. Nuclear Instruments and Methods in Physics Research, Section A: Accelerators, Spectrometers, Detectors and Associated Equipment, 2006, 569, 210-214.	1.6	6
97	Patient and staff radiation dosimetry during cardiac electrophysiology studies and catheter ablation procedures: a comprehensive analysis. Europace, 2006, 8, 443-448.	1.7	70
98	On the response of Y3Al5O12: Ce (YAG: Ce) powder scintillating screens to medical imaging X-rays. Nuclear Instruments and Methods in Physics Research, Section A: Accelerators, Spectrometers, Detectors and Associated Equipment, 2005, 538, 615-630.	1.6	37
99	Light emission efficiency and imaging performance of Y3Al5O12: Ce (YAG: Ce) powder screens under diagnostic radiology conditions. Applied Physics B: Lasers and Optics, 2005, 80, 923-933.	2.2	19
100	Evaluation of ZnS:Cu phosphor as X-ray to light converter under mammographic conditions. Radiation Measurements, 2005, 39, 263-275.	1.4	31
101	Optical gain signal-to-noise ratio transfer efficiency as an index for ranking of phosphor- photodetector combinations used in X-ray medical imaging. Applied Physics A: Materials Science and Processing, 2004, 78, 915-919.	2.3	5
102	Modeling quantum and structure noise of phosphors used in medical X-ray imaging detectors. Nuclear Instruments and Methods in Physics Research, Section A: Accelerators, Spectrometers, Detectors and Associated Equipment, 2002, 490, 614-629.	1.6	33
103	Modeling quantum noise of phosphors used in medical X-ray imaging detectors. Nuclear Instruments and Methods in Physics Research, Section A: Accelerators, Spectrometers, Detectors and Associated Equipment, 1999, 430, 559-569.	1.6	16
104	Effect of intrinsic-gain fluctuations on quantum noise of phosphor materials used in medical X-ray imaging. Applied Physics A: Materials Science and Processing, 1999, 69, 337-341.	2.3	11
105	Estimation of the information content of medical images produced by scintillators interacting with diagnostic X-ray beams. Nuclear Instruments & Methods in Physics Research B, 1999, 155, 199-205.	1.4	3